# Twist defects in helical sonic structures

C. Oldano, J. A. Reyes,* and S. Ponti
*Dipartimento di Fisica, Politecnico di Torino and Istituto Nazionale per la Fisica della Materia (INFM), Corso Duca degli Abruzzi 24, 10129 Torino, Italy*

(Received 20 December 2002; published 27 May 2003)

We analyze theoretically both the acoustic wave propagation in periodic media made of anisotropic materials whose stiffness tensor is uniformly rotating along a given axis $x_3$ and the defect mode produced by twisting about $x_3$ one part of the helical structure with respect to the other. Within the Bragg band of the periodic structure, the twist defect gives rise to a resonant mode that is a superposition of two standing waves: one localized with $\exp(-\gamma|x_3|)$ dependence centered at the defect and the other extended over the whole sample. The ratio between the amplitudes of the localized and nonlocalized waves depends sharply on both the twist angle and the elastic anisotropy, and can assume huge values. The defect mode and the resonance frequency $\omega_0$ are defined by fully analytical and very simple expressions. Finally, we discuss how around $\omega_0$, a finite sample acts as a frequency filter for circularly polarized shear waves, whose bandwidth can be changed by many orders of magnitude by varying the sample thickness, the twist angle, or the elastic anisotropy.

DOI: 10.1103/PhysRevE.67.056624 PACS number(s): 42.70.Qs, 61.30.−v, 62.65.+k

## I. INTRODUCTION

The unique optical properties of cholesteric liquid crystals have been the object of intense research during more than one century. In particular, fully analytic and exact solutions for the electromagnetic wave propagation along the helix axis were independently found by Kats and Nityananda [1,2]. These expressions exhibit the presence of a large frequency gap, where two of the four eigenwaves are nonpropagating. The advances in deposition techniques have allowed to fabricate solid crystals having the same structure as cholesteric liquid crystals and to insert defects for photonic applications. The defects can be generated by inserting an isotropic layer in the middle of a cholesteric liquid crystal sample between planes orthogonal to the periodicity direction $x_3$ [3] and similarly in solid crystals [4,5], or more simply by rotating about $x_3$ one of the two half parts of the sample with respect to the other (twist defects [6–9]).

Solid helical structures made of anisotropic materials whose elastic tensor is uniformly rotating about $x_3$ are also of interest for sonic applications. Ideal structures without defects have been largely treated [10–16], whereas helical structures with defects received smaller attention so far [17,18]. The aim of this paper is the study of the defect modes produced by a twist defect in helical structures and their effects on the acoustical properties of finite samples. Since in helical media the wave equation admits exact and fully analytical solutions, such structures represent an ideal tool for the exact description and the study of defect modes in samples with twist defects, yielding a full understanding of their causes. This paper is organized as follows. In Sec. II, we recall the basic equations for axial propagation in helical structures given in Refs. [10,11]. In Sec. III, we discuss the properties of the shear eigenmodes in a periodic medium without defects, by considering helical structures whose shear (transversal) and compressional (longitudinal) waves are decoupled. The properties of the defect mode are discussed in Sec. IV, and finally in Sec. V the influence of the presence of the twist defect on the transmission and reflection properties of finite samples is examined.

## II. EIGENMODES FOR AXIAL PROPAGATION: BASIC EQUATIONS

Let us first consider solid helical structures without defects, made of anisotropic materials whose elastic tensor rotates uniformly about a given axis $x_3$, thus describing a helix with pitch $p$. For axial propagation of the elastic wave it is convenient to express the components of the displacement vector $\mathbf{u}_d$ and of the stress tensor $\sigma$ in a frame $x_1, x_2, x_3$ rotating solidly with the material structure. In this frame the components $\lambda_{ijmn}$ of the stiffness tensor have constant values and the propagation equation for monochromatic fields of frequency $\Omega$, with a time dependence $\exp(-i\Omega t)$, can be written as

$$\partial_3 \alpha(x_3) = iqH\alpha(x_3), \tag{1}$$

where $H$ is a constant $6\times 6$ matrix, $q=2\pi/p$, $\alpha$ is the six-vector whose elements are the components of the displacement vector $\mathbf{u}_d$ and the components $\sigma_{13}$, $\sigma_{23}$, $\sigma_{33}$ of the stress tensor. It is convenient to introduce the following dimensionless quantities:

$$\mathbf{u} = q\mathbf{u}_d, \quad s_i = \sigma_{i3}/\eta_0,$$

and to define the matrix $H$ as

$$H \equiv \begin{pmatrix} H_{uu} & H_{us} \\ H_{su} & H_{ss} \end{pmatrix},$$

with

*On leave from Instituto de Física, Universidad Nacional Autonoma de Mexico, Apdo P. 20-364, 01000, Mexico D.F., Mexico.

 

$$iH_{uu} \equiv iH_{ss} \equiv \begin{pmatrix} 0 & 1 & 0 \\ -1 & 0 & 0 \\ 0 & 0 & 0 \end{pmatrix},$$

$$iH_{us} \equiv \begin{pmatrix} e_1 & 0 & e' \\ 0 & e_2 & e'' \\ e' & e'' & e_3 \end{pmatrix}, \quad iH_{su} \equiv -\omega^2 \begin{pmatrix} 1 & 0 & 0 \\ 0 & 1 & 0 \\ 0 & 0 & 1 \end{pmatrix}, \tag{2}$$

where $i=1,2,3$, the parameter $\eta_0$ is a suitable average of the elastic compliance, the elements of the submatrix $H_{us}$ are dimensionless quantities (such quantities will be defined below) and $\omega$ is a reduced, dimensionless, angular frequency, given by the equation

$$\omega \equiv \Omega \sqrt{\rho \eta_0}, \tag{3}$$

where $\rho$ is the density of the medium. The propagation equation admits six independent solutions of the type $\beta_j \exp(iqk_j x_3)$, where the state vectors $\beta_j$ and the reduced wave vectors $k_j$ are the eigenvectors and eigenvalues of $H$, respectively, which define the eigenmodes of the acoustic field. It is worthwhile to remind that the simplicity of such plane wave solutions is due to the use of the rotating frame representation. In the laboratory frame the eigenmodes acquire the form of Bloch waves which can be expressed as a superposition of plane waves having reduced wave vectors $(k+1)\hat{\mathbf{x}}_3$, $k\hat{\mathbf{x}}_3$, $(k-1)\hat{\mathbf{x}}_3$, as expected for periodic media.

The properties of the eigenmodes and the shape of the dispersion curves depend on the material parameters, which appear in the submatrix $H_{us}$. Let us restrict our analysis to the case

$$e' = e'' = 0, \tag{4}$$

in which the eigenvalue equation splits into two independent equations, since the longitudinal components $u_3$, $s_3$ are decoupled from the transversal ones. The equation containing $u_3$ and $s_3$ describes compressional waves, while the other represents shear waves and can be written as

$$\begin{pmatrix} 0 & 1 & e_1 & 0 \\ -1 & 0 & 0 & e_2 \\ -\omega^2 & 0 & 0 & 1 \\ 0 & -\omega^2 & -1 & 0 \end{pmatrix} \begin{pmatrix} u_1 \\ u_2 \\ s_1 \\ s_2 \end{pmatrix} = ik \begin{pmatrix} u_1 \\ u_2 \\ s_1 \\ s_2 \end{pmatrix}. \tag{5}$$

If $e_1 \neq e_2$, which means anisotropic behavior of the structure under shear deformation, the transversal components are coupled. In this paper we shall study the solutions of Eq. (5), which are very similar to those of Maxwell's equations for axial propagation of the electromagnetic fields in cholesteric liquid crystals. For such a reason the helical structures satisfying Eq. (4) have been called cholestericlike in Ref. [11].

Equation (4) is satisfied for a medium having $x_1, x_2, x_3$ as symmetry axes (we remind that the periodic medium appears as homogeneous in the rotating frame). If the medium has the same symmetries as hexagonal crystals with the crystallographic axis $z$ parallel to $x_1$, then

$$e_1^{-1} = \eta_0 \lambda_{xzxz}, \quad e_2^{-1} = \eta_0 \lambda_{xyxy}, \quad e_3^{-1} = \eta_0 \lambda_{xxxx}. \tag{6}$$

By considering lossless media and by setting

$$\eta_0 \equiv \frac{1}{2} \frac{\lambda_{xzxz} + \lambda_{xyxy}}{\lambda_{xzxz} \lambda_{xyxy}}, \tag{7}$$

the relation $e_1 + e_2 = 2$ is fulfilled, and we can take

$$e_1 = 1 + e_a, \quad e_2 = 1 - e_a, \tag{8}$$

where $e_a = (e_1 - e_2)/2$ is the anisotropy parameter of interest for cholestericlike structures. However, it must be observed that in lossy media the relation $e_1 + e_2 = 2$ is not satisfied because the imaginary parts of $e_1$ and $e_2$ do not add to zero.

Equation (4) is no longer valid if the crystallographic axis $z$ is obliquely oriented with respect to the helix axis $x_3$, and the structure turns out to be smecticlike. The equations defining the parameters $e_1$, $e_2$, $e_3$, $e'$, $e''$ for smecticlike structures, which are not considered here, are given in Ref. [11] with a slightly different symbolism. Propagation equations equivalent to Eqs. (1) and (5) have also been found and discussed in Ref. [10].

## III. PROPERTIES OF THE SHEAR EIGENWAVES IN CHOLESTERICLIKE STRUCTURES

The eigenvalues and eigenvectors of Eq. (5) are very easily found [10,11]. They are given by the equations

$$k^2 = 1 + \omega^2 \frac{(e_1 + e_2)}{2} \pm \frac{1}{2} \sqrt{8(e_1 + e_2)\omega^2 + (e_1 - e_2)^2 \omega^4}, \tag{9}$$

$$e_1 s_1 = iku_1 - u_2, \quad e_2 s_2 = iku_2 + u_1, \tag{10}$$

$$\frac{u_2}{u_1} = \frac{e_1 e_2 \omega^2 - e_1 - e_2 k^2}{ik(e_1 + e_2)}. \tag{11}$$

For real $e$ values, namely, if the medium is lossless and locally achiral, the eigenvalues $k_j$ are real and given by $\pm k_1$, $\pm k_2$ except for values of $\omega$ within the frequency gap, where $k_1$ is purely imaginary. The dispersion relations of the four transversal eigenmodes $1^+$, $1^-$, $2^+$, $2^-$ and of the longitudinal ones $3^+$ and $3^-$ are plotted in Fig. 1. Notice that only the modes 1 display a frequency gap placed between $\omega_1$ and $\omega_2$, where

$$\omega_1^2 = 1/e_1, \quad \omega_2^2 = 1/e_2.$$

In what follows we shall assume $e_a > 0$ and as a consequence $\omega_2 > \omega_1$.

Before concluding this section, let us stress some features of the eigenmodes which will be useful in our analysis. Equations (11) and (10) show that the ratios $u_2/u_1$ and $s_2/s_1$ are purely imaginary for real values of $k$ so that the waves propagating without attenuation are elliptically polarized. In contrast, these ratios are real for imaginary $k$ and as a result

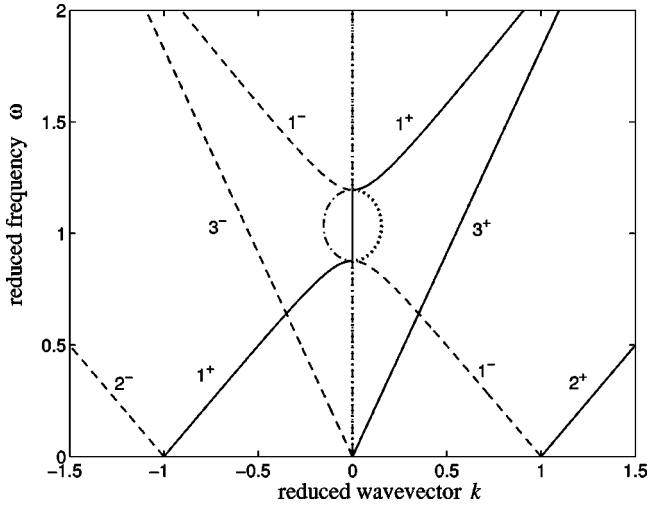


FIG. 1. Dispersion curves in the rotating frame for helical structures without coupling between shear and compressional deformations. The solid and dashed lines refer to the real parts of $k$ for forward and backward modes, respectively; the dash-dotted and dotted lines to the corresponding imaginary parts $1^{\pm}$ and $2^{\pm}$ are shear modes and $3^{\pm}$ compressional modes. In the laboratory frame the curves $3^{\pm}$ are unchanged. The other ones are shifted along the horizontal axis by $+1$ or $-1$ and a new plane wave component with a different value of $k$ appears, because the eigenmodes in periodic media are Bloch waves. In the frequency range where $k$ is purely imaginary the modes $1^{\pm}$ represent surface standing waves. In the presence of coupling between shear and compressional waves, a new frequency gap appears around the intersection point of the curves $1^{+}$, $3^{-}$ and $1^{-}$, $3^{+}$.

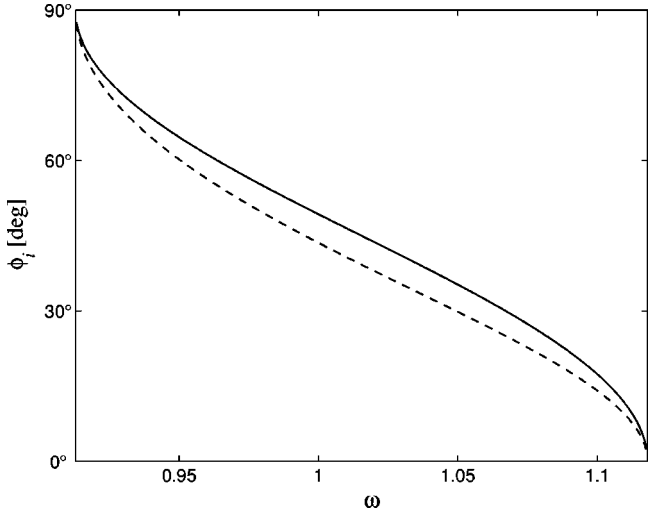


FIG. 2. Angles $\phi_i$ with $i=u,s$, defining the direction of the vectors **u** and **s** for the modes $1^{\pm}$ within the frequency gap for $e_a=0.2$: $\phi_u=\tan^{-1}(u_2/u_1)$ (continuous line), $\phi_s=-\tan^{-1}(s_1/s_2)$ (dashed line). Notice that $\phi_u$ and $\phi_s$ are defined in such a way that at the gap edges, where $\phi_u=\phi_s$, the vectors **u** and **s** are orthogonal. The nonorthogonality of these vectors within the gap influences strongly the shape and the width of the defect mode.

the exponentially attenuated solutions, corresponding to standing waves, are linearly polarized.

At the upper edge of the gap the plane vectors $\mathbf{u}^{+}$ and $\mathbf{u}^{-}$ of the modes $1^{+}$ and $1^{-}$ are parallel to the axis $x_2$ corresponding to the minimum value of $e$. By suitably normalizing the eigenvectors of $H$, $\mathbf{u}^{+}$ and $\mathbf{u}^{-}$ become coincident for $\omega=\omega_2$. By decreasing $\omega$ from $\omega_2$ to $\omega_1$, these vectors rotate monotonically by an angle $\pi/2$ with *opposite senses of rotation*, so that they become antiparallel at the lower edge of the gap. Similarly, the vectors $\mathbf{s}^{+}$ and $\mathbf{s}^{-}$ are parallel to $x_1$ for $\omega=\omega_2$, and rotate by $\pi/2$ becoming antiparallel for $\omega=\omega_1$. Such properties of the nonpropagating solutions are of great importance for the search of the possible localized modes within the frequency gap, as we shall see the following section, which defines the defect mode in lossless media.

## IV. TWIST DEFECT AND DEFECT MODE

Let us now consider two identical semi-infinite cholestericlike structures filling the half spaces $x_3<0$ and $x_3>0$, respectively, the second one rotated by an angle $2\phi$ with respect to the first one. The eigenvectors at the left and right hand sides of the discontinuity plane will be indicated with the letters $\alpha$ and $\beta$, respectively.

For the shear modes 1 and 2 the components $u_3$ and $s_3$ are identically zero. The vectors $\alpha$ and $\beta$ will be written as four-vectors defined by the couples of plane vectors $\mathbf{u}_{\alpha}$, $\mathbf{s}_{\alpha}$ and $\mathbf{u}_{\beta}$, $\mathbf{s}_{\beta}$, respectively. For each eigenmode, the plane vectors **u**, **s** defining $\beta$ are obviously rotated by an angle $2\phi$ with respect to those defining $\alpha$.

In order to define the properties of the defect modes within the frequency gap, it is important to consider the eigenmodes $\alpha_1^{-}$ and $\beta_1^{+}$. As a consequence of the properties discussed in the preceding section, the vectors $\mathbf{u}_{\alpha}^{-}$ and $\mathbf{u}_{\beta}^{+}$ make an angle $2\phi$ for $\omega=\omega_2$, that is, at the upper edge of the frequency gap. By decreasing $\omega$, they rotate in opposite senses, and become coincident for a given angle $\phi_u$, corresponding to a well defined frequency $\omega_u$. Similarly, the vectors $\mathbf{s}_{\alpha}^{-}$ and $\mathbf{s}_{\beta}^{+}$ become coincident at a frequency $\omega=\omega_s$. If $\omega_s=\omega_u$, a physically acceptable solution is given by

$$f(x_3)=f_{\alpha}(x_3)\Theta(-x_3)+f_{\beta}(x_3)\Theta(x_3), \tag{12}$$

where

$$f_{\alpha}(x_3)=\alpha_1^{-}\exp(\gamma x_3), \quad f_{\beta}(x_3)=\beta_1^{+}\exp(-\gamma x_3), \tag{13}$$

$\gamma=qk_1$ and $\Theta(x)$ is the Heaviside step function. In fact, the function $f(x_3)$ satisfies the propagation equation and is continuous at the defect plane, in agreement with the requirement of continuity of the vectors **u** and **s**. The function $f(x_3)$ defines a localized defect mode occurring at the frequency $\omega_u=\omega_s$, as it is evident.

For the helical medium studied here, the functions $\omega_u(\phi)$ and $\omega_s(\phi)$ are very close but not coincident, as shown in Fig. 2 where the inverse functions $\phi_u(\omega)$ and $\phi_s(\omega)$ are plotted. Hence, no physically acceptable solution defining a localized mode exists, since it is impossible to fulfill the requirements of continuity for both vectors **u** and **s**. However, a solution which is continuous at the site defect can be

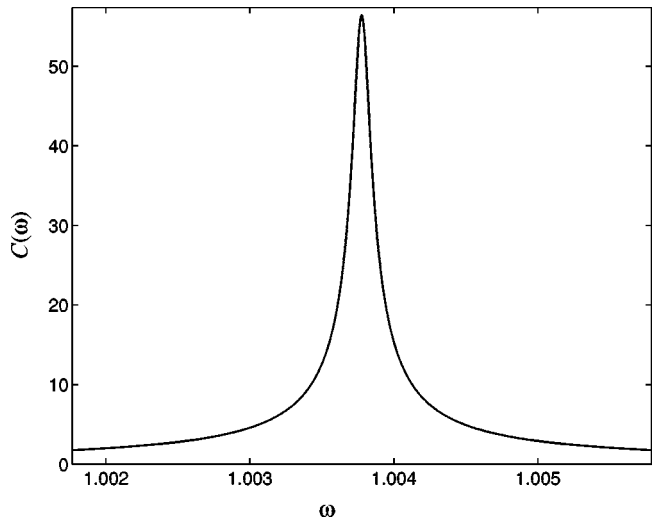


FIG. 3. Amplitude ratio $C(\omega)$ between the localized and the nonlocalized component of the defect mode for a twist defect with twist angle $2\phi=\pi/2$ and anisotropy parameter $e_a=0.1$.

found by adding to each one of the functions $f_\alpha$ and $f_\beta$ a linear combination of the eigenmodes $2^+$ and $2^-$. The new function $f(x_3)$ contains four free parameters, which allow to satisfy the four boundary conditions for the plane vectors **u** and **s**. Symmetry considerations and physical intuition suggest that the amplitudes of the counterpropagating modes $2^+$ and $2^-$ have the same modulus leading as a result to a standing wave. Indeed, for any $\omega$ within the frequency gap a solution exists which can be expressed by the following functions:

$$f_\alpha = C\alpha_1^- \exp(\gamma x_3) + \exp(-i\delta)\alpha_2^+ \exp(iqk_2x_3) + \exp(i\delta)\alpha_2^- \exp(-iqk_2x_3),$$

$$f_\beta = C\beta_1^+ \exp(-\gamma x_3) + \exp(i\delta)\beta_2^+ \exp(iqk_2x_3) + \exp(-i\delta)\beta_2^- \exp(-ik_2x_3), \quad (14)$$

where the phase angle $\delta$ depends on the normalization of the eigenvectors. The eigenvectors $\alpha_2^\pm$ and $\beta_2^\pm$ have been normalized to unit power flux $P$, which is given by

$$P=\beta^\dagger M\beta, \quad M=\frac{1}{2}\begin{pmatrix} 0 & 0 & -i\omega & 0 \\ 0 & 0 & 0 & -i\omega \\ i\omega & 0 & 0 & 0 \\ 0 & i\omega & 0 & 0 \end{pmatrix}, \quad (15)$$

where the superscript † denotes the Hermitian conjugation. The eigenmode $\alpha_1^-$, which represents a standing wave with $P=0$, has been normalized by setting

$$|(\alpha_1^+)^\dagger M\alpha_1^-|=1, \quad (16)$$

and similarly for $\beta_1^+$. The amplitude $C$ of the localized component of the defect mode depends strongly on $\omega$. In fact, the function $C(\omega)$, depicted in Fig. 3, exhibits an enhanced maximum at a frequency $\omega=\omega_0$ depending on the twist angle $2\phi$. For a given value of $\phi$, $\omega_0$ is located between the frequencies $\omega_u$ and $\omega_s$. A monotonic dependence of $\omega_0$ on $\phi$ has already been evidenced in Ref. [17], which gives the transmittance of samples with different $\phi$ values. We have found a fully analytic equation relating $\omega_0$ and $\phi$, which can be written as

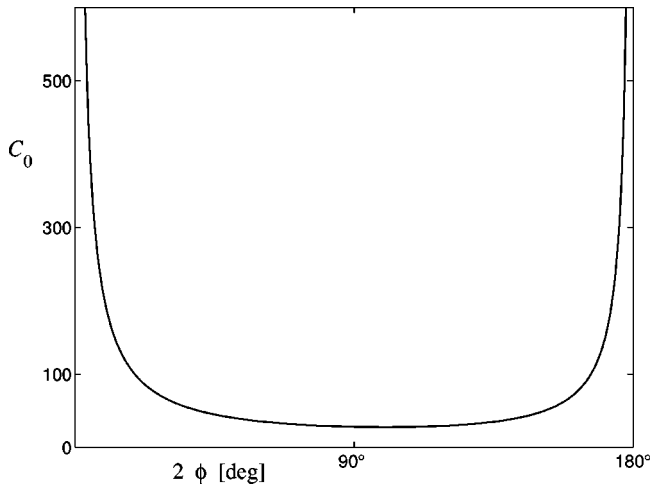


FIG. 4. Maximum value of $C(\omega)$, $C_0=C(\omega_0)$, as a function of the twist angle $2\phi$ for $e_a=0.2$.

$$2\phi=\pi-\phi_u-\phi_s, \quad (17)$$

where

$$\phi_u=\tan^{-1}\left(\frac{e_1e_2\omega_0^2-e_1-e_2k_1^2}{2ik_1}\right),$$

$$\phi_s=-\tan^{-1}\left(\frac{e_2}{e_1}\frac{ik_1-\tan\phi_u}{ik_1\tan\phi_u+1}\right). \quad (18)$$

Here $k_1$ is the function of $\omega_0$ defined by the dispersion relation (9). The maximum value $C_0=C(\omega_0)$ of the function $C(\omega)$ depends on the twist angle $2\phi$ and on the elastic anisotropy $e_a$, as shown in Figs. 4 and 5, respectively. One

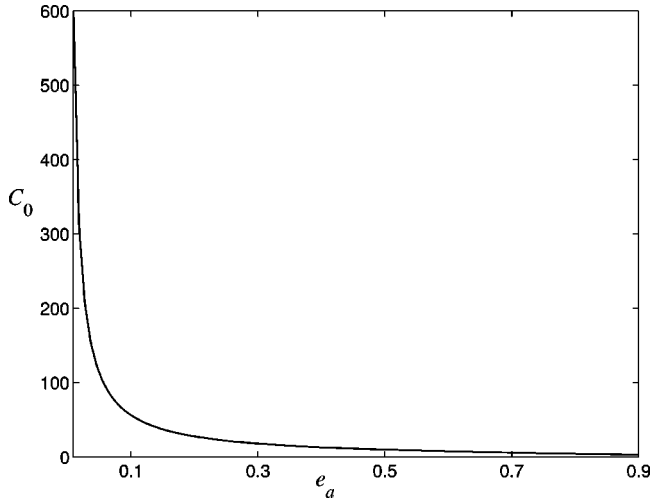


FIG. 5. $C_0$ versus $e_a$ for a twist angle $2\phi=\pi/2$.

may notice that $C_0$ increases dramatically when $\omega_0$ approaches to the gap edges $\omega_1$ and $\omega_2$, or when the elastic anisotropy $e_a$ decreases.

## V. PROPERTIES OF SAMPLES WITH TWIST DEFECTS

A finite sample between the planes $x_3=-l_a$ and $x_3=l_b$, with a twist defect located at $x_3=0$, behaves as a resonant cavity whose properties depend on $l_a$, $l_b$, $\phi$, and $e_a$. The $\mathcal{Q}$ factor and the phonon dwell time can reach very high values by appropriately choosing such parameters.

In order to analyze the properties of the sample, it is convenient to express the acoustic fields within and outside the sample as a superposition of eigenmodes so that we can make use of the scattering-matrix formalism. We consider first the scattering matrix associated with the defect plane. It can be defined by the relation

$$a_{out}=Sa_{inc}, \tag{19}$$

where $a_{out}$ and $a_{inc}$ are four-vectors whose elements are the amplitudes of the outgoing and incoming eigenwaves, which will be ordered as follows: $\beta_1^+$, $\beta_2^+$, $\alpha_1^-$, $\alpha_2^-$ and $\alpha_1^+$, $\alpha_2^+$, $\beta_1^-$, $\beta_2^-$, respectively. Thus, the element $S_{11}$ provides the amplitude of the mode $\beta_1^+$ generated by an incident signal entering from the left hand side of the defect plane and containing the unit amplitude mode $\alpha_1^+$. In general, the elements $S_{ij}$ with $j=1,2$ furnish the transmission properties of the defect plane when $i=1,2$ and the reflection properties when $i=3,4$, for waves coming from the left hand side. The quantities $|S_{ij}|$ are plotted in Fig. 6 as a function of $\omega$. The upper curves refer to a lossless medium, (a0) refers to the standing waves 1, giving its transmission ($i=j=1$) and reflection ($i=3$, $j=1$) properties, (c0) refers to the propagating waves 2, (b0) to the mode exchanging. Note that the two curves plotted in (a0) are practically coincident and reach a remarkable maximum at the resonant frequency $\omega_0$, showing that for $\omega=\omega_0$ the wave $1^+$ gives rise to new transmitted and reflected waves $1^\pm$ with huge amplitude. A similar behavior is displayed by the curves plotted in (b0), but here the maximum is less pronounced. The dashed curve in (c0) shows that the defect plane reflects totally the propagating eigenmode $2^+$ at the frequency $\omega_0$.

The other curves ($ai$), ($bi$), and ($ci$) ($i=1,2$) plotted in Fig. 6 are similarly defined, but they refer to lossy media. One may notice that a very small imaginary part of $e_1$ and $e_2$ has dramatic effects on the scattering properties of the defect plane. The dissipation also changes the properties of the eigenmodes $1^\pm$, which become elliptically polarized because in Eqs. (10) and (11) the reduced eigenvalue $k$ is no more purely imaginary. Further, also the eigenmodes $2^\pm$ become exponentially attenuated, a fact that can greatly change the properties of thick samples. However, the optical properties of dissipative samples with a twist defect are dominated by the effects shown in Fig. 6. A satisfactory theory including dissipation becomes very involved. Therefore in the following only nondissipative samples will be considered.

The curves plotted in Fig. 6 imply that any incident wave on the discontinuity plane generates a defect mode with large

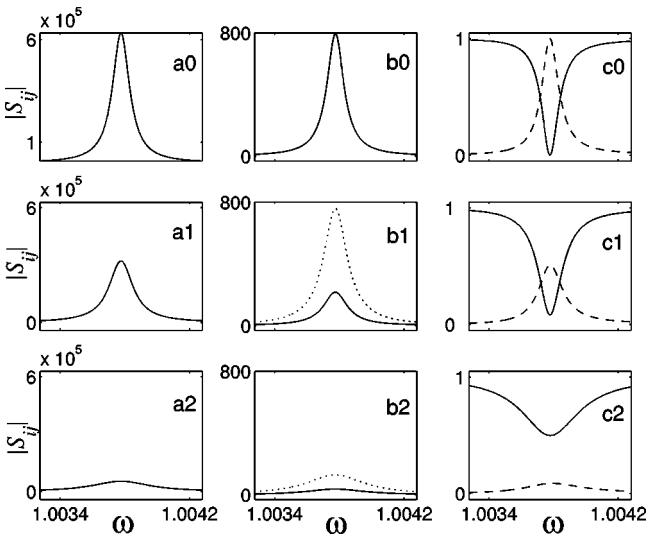


FIG. 6. $|S_{ij}|$ versus $\omega$, where $S$ is the scattering matrix of the defect plane, for $2\phi=\pi/2$. ($ai$) $|S_{11}|$ and $|S_{31}|$, ($bi$) $|S_{21}|$, $|S_{12}|$, $|S_{41}|$ and $|S_{32}|$, ($ci$) $|S_{22}|$ and $|S_{42}|$, where the indices 1 and 3 refer to the standing waves, 2 and 4 to the propagating ones, the solid and dashed lines refer to transmitted and reflected waves, respectively. The index $i$, with $i=0,1,2$, corresponds to media where the parameters $e_1$,$e_2$ have real parts equal to 1.1 and 0.9, respectively, and different imaginary parts: 0 for $i=0$; $0.5\times10^{-4}$ for $i=1$; and $3\times10^{-4}$ for $i=2$. The curves plotted in (a0), (a1), (a2), and (b0) are practically coincident, whereas in (b1) and (b2) the quantities $|S_{12}|$ and $S_{32}$ (dotted lines) are quite different from $|S_{21}|$ and $S_{41}$ (full lines). Notice the different scales in the vertical axes.

amplitude and that the exponentially decaying eigenwaves are much more efficient than the propagating ones in generating the resonant defect mode. However, it should be observed that the attenuated wave $1^+$ is originated at the sample boundary $z=-l_a$ and vanishes before reaching the defect site if $l_a \gg l_c$, where

$$l_c=(qk_1)^{-1}=\frac{p}{2\pi|k_1|}$$

is its characteristic length. On the basis of the above considerations, it is now quite easy to understand the reflection and transmission properties of finite samples without dissipation. We shall consider a sample with $l_a=l_b=l$, immersed in an isotropic medium. The polarization properties of the transmitted and reflected waves at the boundary planes $z=-l$ and $z=l$ depend on the impedance mismatch of the two media, which is minimized if the $e$ value of the external medium lies between $e_1$ and $e_2$, and when $e_1 \sim e_2$. Under these conditions, the eigenmodes 1 and 2 are excited by waves whose shear polarization is nearly circular. More precisely, right circularly (RC) and left circularly (LC) polarized waves excite, respectively, the eigenwaves 1 and 2 in cholestericlike samples with right handed helix. The transmittance and reflectance of samples with $e_a=0.1$, $2\phi=\pi/2$, and different $l$ values are plotted in Fig. 7. To clarify the role of the twist defect, we should remind that in the limit of the zero impedance mismatch, right handed samples without defects and

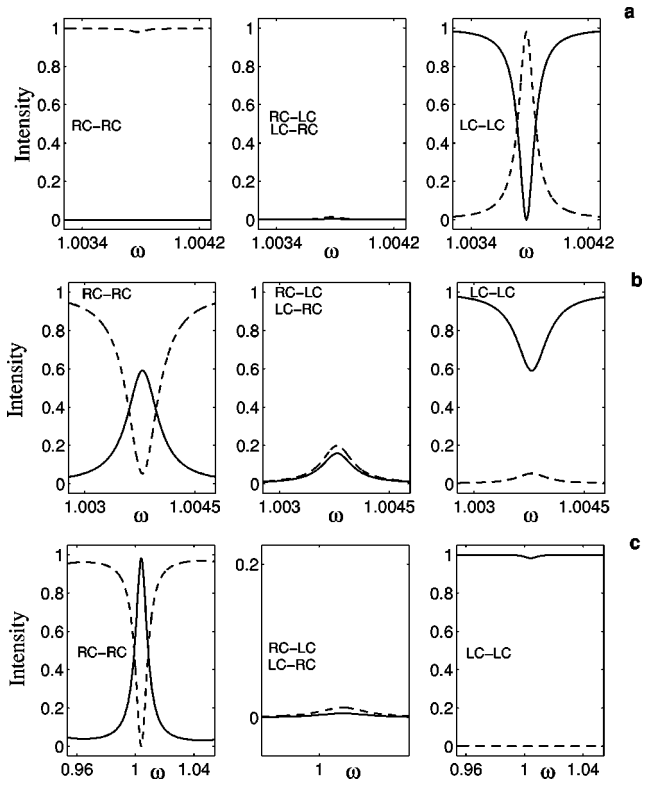


FIG. 7. Transmittance (continuous lines) and reflectance (dashed lines) curves versus the normalized frequency $\omega$ for circularly polarized waves in samples with elastic anisotropy $e_a=0.1$, twist angle $2\phi=\pi/2$, and different thicknesses: (a) $l=2\pi l_c$, (b) $l=\pi l_c$, and (c) $l=\pi l_c/2$. The sample is immersed within an isotropic medium with $e=1$.

thickness $l>l_c$ transmit totally LC waves and reflect RC waves. The curves of Fig. 7(a), corresponding to $l=2\pi l_c$, are now easily understood. The twist defect plays no role for the RC wave, that vanishes before reaching the defect plane, whereas it reflects the LC wave only in a narrow interval of frequency around $\omega_0$, in agreement with the previously found results illustrated in Fig. 6(c0). Thus, thick samples act as frequency filters for circularly polarized waves giving peaks in reflection and holes in transmission. The presence of narrow holes in transmission has already been evidenced in Ref. [17], where samples with twist defects are considered, in the framework of a previously developed theory concerning a three-layer system [18].

One may notice that the width of the LC-LC peaks and holes plotted in Fig. 7(a) and in Fig. 6(c0) are practically coincident. This is a consequence of the fact that in thick samples the coupling of the defect mode with the external radiation field is only due to the nonlocalized component. The high $Q$ factor of thick samples is a consequence of the fact that the amplitude of such component is very small, as shown in Figs. 3–5. By decreasing the sample thickness the amplitude of the localized component at the boundary plane increases exponentially. For $l=\pi l_c$ its contribution to the rate of energy loss is nearly equal to the previous one [Fig. 7(b)] and it becomes dominant for $l=\pi l_c/2$ [Fig. 7(c)], thus greatly decreasing the $Q$ factor and correspondingly increasing the linewidth of peaks and holes. The presence of RC-RC peaks and holes in the plots of Figs. 7(b) and 7(c) is evidently due to the fact that the amplitude of the mode $1^+$ at the defect site is no more negligibly small and such to excite a defect mode with huge amplitude, in agreement with Fig. 6(a0). For $l<l_c$ it could not be convenient to define the sample properties on the basis of properties of the defect mode discussed in Sec. IV, which have been found by considering the limit $l\to\infty$, because in thin samples also the modes $\alpha_1^+$ and $\beta_1^-$ must be taken into account. Such properties can be found by considering the scattering properties of the discontinuity planes and the properties of the eigenmodes $1^\pm$ and $2^\pm$, or by using methods similar to those of Ref. [5].

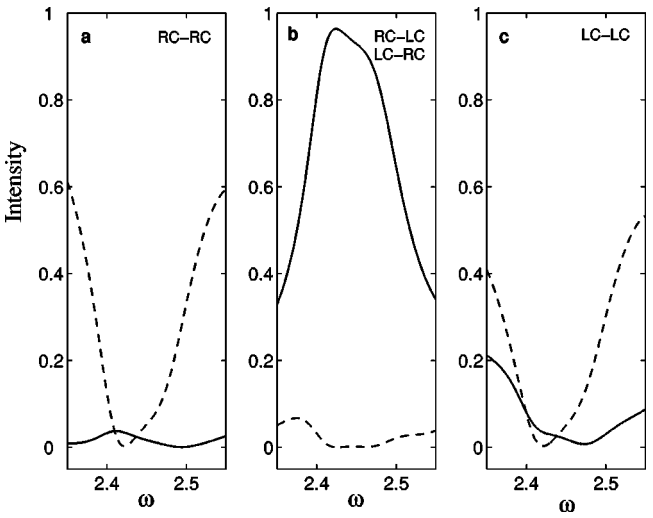


FIG. 8. The same as in Fig. 7, for $e_a=0.75$, $2\phi=114°$, $\omega=\omega_0$, and $l=5l_c$.

Figure 7(b) shows LC-RC and RC-LC mode conversion peaks. The height of these peaks depends strongly on the sample parameters. By suitably choosing such parameters the incident energy can be totally converted in the orthogonal polarization state, as shown in Fig. 8(b).

The possibility to generate a standing wave having huge energy density around the defect site using weak external waves is of great interest for applications concerning nonlinear effects.

## VI. CONCLUDING REMARKS

We conclude by addressing the following comments.

(i) We considered a helical structure without coupling between longitudinal and transversal deformations. The acoustic properties of the transversal waves are very similar to the optical properties of cholesteric liquid crystals, which have been the object of a great deal of research. In particular, optical RC-RC and LC-LC transmittance and reflectance curves similar to those shown in Fig. 7 are given in Ref. [6] without a clear explanation. We gave an explanation of the acoustical effects generated by the twist defect, which should have an optical equivalent, as it is evidently expected. To the best of our knowledge, such analysis was given here for the first time. Specifically, we were able to exactly define the

defect mode, to give a simple equation for the resonance frequency and to thoroughly describe its origin.

(ii) The defect mode contains a nonlocalized component, which vanishes in the limit of zero anisotropy or for twist angles equal to zero or $\pi$, that is to say, under the conditions when the twist defect disappears. The presence of a nonlocalized part is necessary because the vectors **u** and **s**, being the acoustical equivalent of the electromagnetic vectors **E** and **H**, are not perfectly orthogonal in the considered helical structures. As a consequence, it is impossible to satisfy the boundary conditions at the defect plane by only taking into account the exponentially decaying solutions present within the frequency gap. In other words, the true control parameter for the width of the resonant mode is the angle between **u** and **s**, which in the helical structure considered here depends only on either the anisotropy of the medium or the twist angle. It is now possible to look for other possible control parameters, for acoustical as well as optical applications.

(iii) Our investigation deserves a continuation in many directions as those we state now: the optical equivalent of the results addressed here, the analysis of helical systems with coupling between shear and compressional waves, which are expected to exhibit conversion between transversal and longitudinal modes, the search of new applications, and a more detailed study of lossy media. Even though many optical applications of the resonant mode have been already discussed in the literature, we believe that our analysis is such to stimulate new research.

[1] E.I. Kats, Zh. Eksp. Teor. Fiz. **59**, 1854 (1970) [Sov. Phys. JETP **32**, 1004 (1971)].
[2] R. Nityananda, Mol. Cryst. Liq. Cryst. **21**, 315 (1973).
[3] Y.C. Yang, C.S. Kee, J.E. Kim, H.Y. Park, J.C. Lee, and Y.J. Chon, Phys. Rev. E **60**, 6852 (1999).
[4] A. Lakhtakia and M. McCall, Opt. Commun. **168**, 457 (1999).
[5] I.J. Hodgkinson, Q.H. Wu, A. Lakhtakia, and M.W. McCall, Opt. Commun. **177**, 79 (2000).
[6] V.I. Kopp and A.Z. Genack, Phys. Rev. Lett. **89**, 033901 (2002).
[7] V.I. Kopp, P.V. Shibaev, R. Bose, and A.Z. Genack, Proc. SPIE **4655**, 141 (2002).
[8] I.J. Hodgkinson, Q.H. Wu, K.E. Thorn, A. Lakhtakia, and M.W. McCall, Opt. Commun. **184**, 57 (2000).
[9] F. Wang and A. Lakhtakia, Opt. Commun. **215**, 79 (2003).
[10] S.F. Nagle, A. Lakhtakia, and W.J. Thompson, J. Acoust. Soc. Am. **97**, 42 (1995).
[11] C. Oldano and S. Ponti, Phys. Rev. E **63**, 011703 (2000).
[12] A. Lakhtakia, K. Robbie, and M.J. Brett, J. Acoust. Soc. Am. **101**, 2052 (1997).
[13] A. Lakhtakia and M.W. Meredith, Sens. Actuators A-Phys. **73**, 193 (1999).
[14] A. Lakhtakia and R. Messier, Mater. Res. Innovations **1**, 145 (1997).
[15] N. Cherradi, A. Kawasaki, and M. Gasik, Composites Eng. **4**, 883 (1994).
[16] Y.Y. Li and L. Chen, Phys. Rev. B **36**, 9507 (1987).
[17] A. Lakhtakia, Sens. Actuators A **80**, 216 (2000).
[18] A. Lakhtakia, Sens. Actuators A **87**, 78 (2000).